REPORT

Heterozygous Mutations in *OAS1* Cause Infantile-Onset Pulmonary Alveolar Proteinosis with Hypogammaglobulinemia

Kazutoshi Cho,[1,11,*] Masafumi Yamada,[2,11] Kazunaga Agematsu,[3] Hirokazu Kanegane,[4] Noriko Miyake,[5] Masahiro Ueki,[2] Takuma Akimoto,[1] Norimoto Kobayashi,[6] Satoru Ikemoto,[7] Mishie Tanino,[8] Atsushi Fujita,[5] Itaru Hayasaka,[1] Satoshi Miyamoto,[4] Mari Tanaka-Kubota,[4] Koh Nakata,[9] Masaaki Shiina,[10] Kazuhiro Ogata,[10] Hisanori Minakami,[1] Naomichi Matsumoto,[5] and Tadashi Ariga[2]

Pulmonary alveolar proteinosis (PAP) is characterized by accumulation of a surfactant-like substance in alveolar spaces and hypoxemic respiratory failure. Genetic PAP (GPAP) is caused by mutations in genes encoding surfactant proteins or genes encoding a surfactant phospholipid transporter in alveolar type II epithelial cells. GPAP is also caused by mutations in genes whose products are implicated in surfactant catabolism in alveolar macrophages (AMs). We performed whole-exome sequence analysis in a family affected by infantile-onset PAP with hypogammaglobulinemia without causative mutations in genes associated with PAP: *SFTPB*, *SFTPC*, *ABCA3*, *CSF2RA*, *CSF2RB*, and *GATA2*. We identified a heterozygous missense variation in *OAS1*, encoding 2′5′-oligoadenylate synthetase 1 (OAS1) in three affected siblings, but not in unaffected family members. Deep sequence analysis with next-generation sequencing indicated 3.81% mosaicism of this variant in DNA from their mother's peripheral blood leukocytes, suggesting that PAP observed in this family could be inherited as an autosomal-dominant trait from the mother. We identified two additional *de novo* heterozygous missense variations of *OAS1* in two unrelated simplex individuals also manifesting infantile-onset PAP with hypogammaglobulinemia. PAP in the two simplex individuals resolved after hematopoietic stem cell transplantation, indicating that OAS1 dysfunction is associated with impaired surfactant catabolism due to the defects in AMs.

Lung surfactant is synthesized and stored in alveolar type II epithelial cells.[1] It is secreted into the alveolar spaces and reduces surface tension at air-liquid interfaces. Surfactant proteins (SP)-B and SP-C are highly hydrophobic and essential for the surface activity of lung surfactant.[2] ATP-binding cassette A3 (ABCA3) transports surfactant phospholipids into lamellar bodies where they bind SP-B and SP-C to form surfactant.[3] Secreted lung surfactant is partially recycled by type II epithelial cells, and the remainder is taken up and catabolized by alveolar macrophages (AMs). Granulocyte-macrophage colony-stimulating factor (GM-CSF) is implicated as essential for catabolism of lung surfactant, as well as the proliferation and maturation of human AMs.[4]

Pulmonary alveolar proteinosis (PAP) is caused by lung surfactant system homeostasis dysfunction[5] and can be categorized into four types: autoimmune PAP (APAP) (MIM: 610910), secondary PAP (SPAP), genetic PAP (GPAP), and unclassified PAP. APAP is caused by excess production of autoantibodies against GM-CSF.[6] AMs of APAP-affected individuals show a typical foamy appearance.[7] SPAP is associated with underlying malignancies or blood diseases, such as myelodysplastic syndrome (MIM: 614286).[8] GPAP is caused by mutations in several genes.[9,10] SP-B, encoded by one of the genes associated with GPAP, *SFTPB* (MIM: 178640), is required for the maturation of SP-C. SP-B deficiency (MIM: 265120) is an autosomal-recessive disease characterized by respiratory distress syndrome (RDS) (MIM: 267450) at birth, which then develops into infantile type PAP.[11] Abnormalities in SP-C (encoded by *SFTPC* [MIM: 178620]) (MIM: 610913) and ABCA3 (encoded by *ABCA3* [MIM: 601615]) (MIM: 610921) are likely to yield manifestations of GPAP and interstitial pneumonitis.[12–14] Mutations in genes encoding GM-CSF receptor (*CSF2RA* [MIM: 306250] and *CSF2RB* [MIM: 138981]) are also associated with GPAP (MIM: 300770, 614370) in infants and adults.[15–17] Mutations in *GATA2* (MIM: 137295) are associated with monocytopenia and mycobacterial infection (MonoMAC) syndrome (MIM: 614172), which shows a broad spectrum of clinical manifestations, including PAP.[18]

In this study, we performed whole-exome sequence (WES) analysis in a family affected by infantile-onset PAP with hypogammaglobulinemia that had no causative mutations in genes associated with PAP: *SFTPB*, *SFTPC*, *ABCA3*, *CSF2RA*, *CSF2RB*, and *GATA2*. In addition, we

[1]Maternity and Perinatal Care Center, Hokkaido University Hospital, Sapporo 060-8648, Japan; [2]Department of Pediatrics, Faculty of Medicine and Graduate School of Medicine, Hokkaido University, Sapporo 060-8638, Japan; [3]Department of Infection and Host Defense, Graduate School of Medicine, Shinshu University, Matsumoto 390-8621, Japan; [4]Department of Pediatrics and Developmental Biology, Tokyo Medical and Dental University, Tokyo 113-8519, Japan; [5]Department of Human Genetics, Yokohama City University Graduate School of Medicine, Yokohama 236-0004, Japan; [6]Department of Pediatrics, Shinshu University School of Medicine, Matsumoto 390-8621, Japan; [7]Division of General Pediatrics, Saitama Children's Medical Center, Saitama 330-8777, Japan; [8]Department of Cancer Pathology, Faculty of Medicine and Graduate School of Medicine, Hokkaido University, Sapporo 060-8638, Japan; [9]Bioscience Medical Research Center, Niigata University Medical & Dental Hospital, Niigata 951-8520, Japan; [10]Department of Biochemistry, Yokohama City University Graduate School of Medicine, Yokohama 236-0004, Japan
[11]These authors contributed equally to this work
*Correspondence: chotarou@med.hokudai.ac.jp
https://doi.org/10.1016/j.ajhg.2018.01.019.

Table 1. Demographic Characteristics of Five Affected Individuals in This Study

	A-II-1	A-II-3	A-II-4	B-II-1	C-II-1
Consanguineous parents	no	no	no	no	no
Gestation (weeks)	38	36	39	39	39
Birth weight (g)	2,896	2,852	2,290	2,140	3,410
Gender	male	male	female	female	female
Age at HSCT	not done	151 d	not done	8 m	11 m
Diagnosis of PAP	AU	BAL+AU	BAL+AU	BAL	BAL
Recurrent infection with hyperreactivity	unknown	unknown	yes	yes	yes
Hypogammaglobulinemia	unknown	unknown	yes	yes	yes
Leukocytosis with normal distribution	yes	yes	yes	yes	yes
Splenomegaly before treatment	yes	yes	yes	unclear	yes
Small and non-foamy AMs	yes	yes	yes	unclear	yes
Age at onset of respiratory dysfunction	39 d	39 d	49 d	2 m	5 m
Respiration status at birth	well	well	well	well	well
Respiration status after BAL	not done	unchanged	unchanged	improved	unchanged
Respiration status after IVIG	unknown	unknown	improved	improved	improved
Outcome	dead/91 d	dead/163 d	dead/11 y	dead/3 y	alive/19 m
Cause of death	respiratory failure	respiratory failure	respiratory failure	renal failure	alive

Abbreviations: AU, autopsy; BAL, bronchoalveolar lavage; HSCT, hematopoietic stem cell transplantation; d, day; m, month; y, year.

further studied two unrelated simplex individuals that also presented with infantile-onset PAP with hypogammaglobulinemia. A summary and details of the affected individuals are shown in Table 1 and Supplemental Note.

This study was conducted in accordance with the Declaration of Helsinki and the national ethical guidelines, and was approved by the Ethics Committees of Hokkaido University Faculty of Medicine and Graduate School of Medicine (16-001), Yokohama City University Graduate School of Medicine, and Tokyo Medical and Dental University. Parents of all individuals included in the study provided written informed consent for genetic analyses and publication. The genomic DNA of two affected siblings (A-II-1 and A-II-3) from family A was extracted by phenol/chloroform methods and stored at –80°C (Figure S1A). The genomic DNA samples of other family members were extracted from heparinized peripheral blood samples using SepaGene (Sankojunyaku). All DNA samples were amplified with an Illustra GenomiPhi DNA Amplification Kit (GE Healthcare). In addition, we established Epstein-Barr virus-transformed lymphoblastoid cell lines (EBV-LCL) from the two siblings, one affected (A-II-4) and one unaffected (A-II-2), and extracted their DNA. WES analysis was performed as described previously.[19] Briefly, 3 μg of whole-genome amplified DNA from peripheral blood or DNA samples from EBV-LCL were used in sample preparation. Genome partitioning was performed with SureSelect Human All Human Exon v4 (Agilent Technology) according to the manufacturer's protocol. The samples were run on a HiSeq2000 (Illumina) with 101-bp paired-end reads and 7-bp index reads. Reads were mapped to the human reference genome (GRCh37.1/hg19) by Novoalign 2.08.02. Variants were called with Genome Analysis Toolkit v1.6-5 and annotated using ANNOVAR (2012feb).

To identify the causative variants, we selected variants based on the following criteria. For the autosomal-dominant (*de novo*) model, we first removed synonymous variants and then selected (1) variants not found in our in-house exome data (n = 153 controls), (2) variants not registered in dbSNP 135 (see Web Resources) or NHLBI Exome Sequencing Project (ESP5400) (see Web Resources), (3) variants outside segmental duplication, (4) variants not observed in either parents or an unaffected sibling, and (5) variants shared among all three affected children. For the homozygous model, we first removed synonymous variants and then selected (1) rare variants ($n \leq 1/153$) in our in-house exome data, (2) variants with minor allele frequency (MAF) ≤ 0.01 in ESP5400, (3) variants outside segmental duplication, and (4) variants shared in three affected children. For autosomal compound heterozygous variants, we first removed synonymous variants and then selected (1) rare variants ($n \leq 1/153$) in our in-house exome data, (2) variants with MAF ≤ 0.01 in ESP5400, (3) variants outside segmental duplication, and (4) variants shared among three affected children. To estimate the mosaic variation in their parents, we counted the reads with variation using the BAM file with Integrative Genomic Viewer (see Web Resources). To confirm the presence of the variant allele in peripheral blood, we sequenced

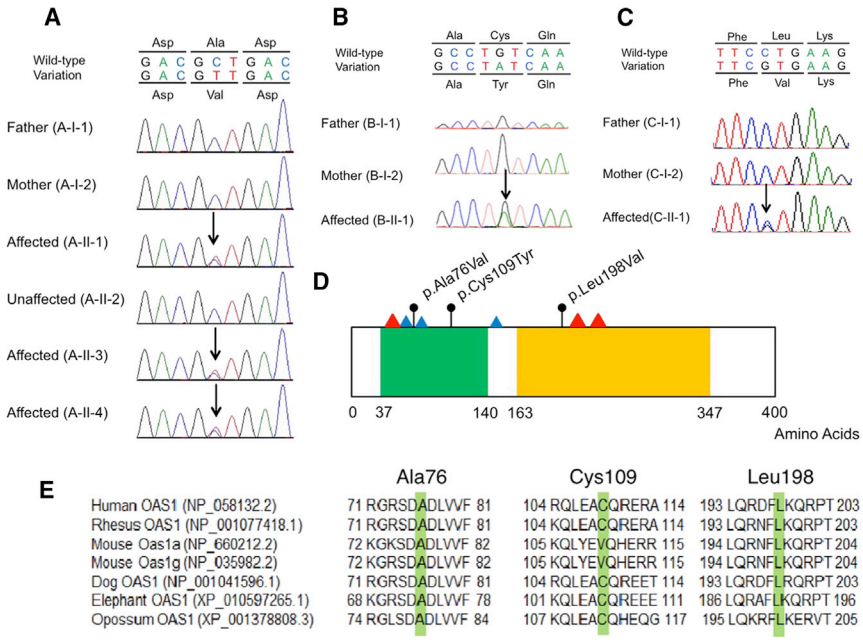

Figure 1. *OAS1* Variants in Three Families with PAP and Evolutionary Conservation and Variations in *OAS1*

(A–C) Genetic analysis for *OAS1* variation. Sanger sequencing demonstrated variations of (A) c.227C>T (p.Ala76Val) in family A, (B) c.326G>A (p.Cys109Tyr) in family B, and (C) c.592C>G (p.Leu198Val) in family C. Black arrows show the positions of the variations.

(D) Schematic representation of *OAS1* mutations. Black circles indicate the variants identified in this study. Blue and red triangles indicate metal binding sites (Asp75, Asp77, and Asp148) and ATP binding sites (Ser63, Lys213, and Gln229), respectively. Green and yellow boxes show the nucleotidyltransferase (NTP_transf_2) domain and 2′,5′-oligoadenylate synthetase 1, domain 2, and C terminus (OAS1_C) domain, respectively, predicted using the SMART program (see Web Resources).

(E) Evolutionary conservation of Ala76, Cys109, and Leu198 amino acids in human OAS1. These amino acids are highlighted in green. Six orthologous sequences were aligned using the multiple sequence alignment program, Clustal Omega (see Web Resources).

the 151-bp amplicon covering the candidate *OAS1* (MIM: 164350) variant by deep sequence analysis using MiSeq with Miseq Reagent Kit v1 (300 cycles) (Illumina). Genomic DNA samples from two unrelated simplex individuals from families B and C (B-II-1 and C-II-1) (Figures S1B and S1C) were subjected to PCR amplification of *OAS1* with primers to cover three transcriptional variants sharing the same exons 1 to 4 (RefSeq: NM_016816.3, NM_002534.3, and NM_001032409.2) as listed in Table S1. Direct sequence analysis of *OAS1* was performed as described previously.[20] Nucleotide sequences were compared with the reported reference sequence of *OAS1* (RefSeq: NM_016816.3).

The quality of WES performance is summarized in Table S2. The exonic regions were not well covered using the whole-genome amplified samples (64.6%–89.6% of coding sequences by ≥20× reads). Although we first considered that the condition in family A was inherited in an autosomal-recessive manner, there were no causative recessive variants (Tables S3 and S4). Unexpectedly, one *de novo* missense variant, c.227C>T (p.Ala76Val) in *OAS1* (RefSeq: NM_016816.3), was shared by all three affected individuals but not by unaffected family members (Figure 1A and Table S5). This variant was not registered in the ESP5400, Exome Aggregation Consortium, or Human Genetic Variation Database and was predicted to be "tolerated" by SIFT and "polymorphism" by MutationTaster, but "probably damaging" by PolyPhen-2 (see Web Resources) (Table 2). This amino acid is located between the metal binding sites (Asp75 and Asp77) in the NTP_transf_2 domain (Figure 1D) and is evolutionarily conserved from opossum to human (Figure 1E). Biological parentage was confirmed based on nine microsatellite markers. As either of the parents could have this variant as a mosaic, we performed deep sequencing of the parents' amplicons covering this variant and detected the mutant T allele at a frequency of 3.81% in the mother (Table S6).

Furthermore, we found two additional heterozygous *OAS1* variants occurring *de novo* in two unrelated simplex individuals with infantile-onset PAP with hypogammaglobulinemia (B-II-1 and C-II-1) (Figures S1B and S1C). A variation of c.326G>A (p.Cys109Tyr) in *OAS1* was observed in B-II-1 but not in her parents (Figure 1B). This missense variation was "tolerated" by SIFT and "polymorphism" by MutationTaster, but "possibly damaging" by PolyPhen-2 (Table 2). Another variation of c.592C>G (p.Leu198Val) in *OAS1* (observed in C-II-1 but not in her parents) (Figure 1C) was predicted as "tolerated" by SIFT, "benign" by PolyPhen-2, and "polymorphism" by MutationTaster (Table 2). Neither p.Cys109Tyr nor p.Leu198Val are included in ESP5400, Exome Aggregation Consortium, or Human Genetic Variation Database.

To assess the impact of p.Ala76Val, p.Cys109Tyr, and p.Leu198Val on protein structure, we mapped these variations onto the crystal structures of a double-stranded RNA (dsRNA)-bound form of human OAS1 (hOAS1) and an apo form of porcine oligoadenylate synthetase 1 (pOAS1) (PDB: 4ig8 and 1px5, respectively) (Figure 2A).[21,22] There are structural differences between the RNA-bound and apo forms. The conformation of OAS1 is stabilized in a catalytically active form, which is capable of binding to ATP and Mg^{2+} ions upon binding to dsRNA. Ala76 in hOAS1 (Ala75 in pOAS1) adjoins the two active site aspartic acid residues, Asp75 and Asp77 (Asp74 and Asp76

Table 2. *OAS1* Mutations Identified in Three Unrelated Families with GPAP

Variants	Prediction Software			Grantham Score
	SIFT	PolyPhen-2	MutationTaster	
c.227C>T (p.Ala76Val)	0.08 (tolerated)	0.936 (probably damaging)	polymorphism	64
c.326G>A (p.Cys109Tyr)	0.18 (tolerated)	0.715 (possibly damaging)	polymorphism	194
c.592C>G (p.Leu198Val)	1.00 (tolerated)	0.349 (benign)	polymorphism	32

in pOAS1), which bind to Mg^{2+} ions. The side chain of Ala76 is involved in a hydrophobic core that would define the active site structure in the RNA-bound form, indicating that the p.Ala76Val variant would affect enzymatic activity. There are structural differences around Cys109 between the RNA-bound and apo forms. The side chain of Cys109 in hOAS1 (Cys108 in pOAS1) is involved in a hydrophobic core of the apo form of OAS1, which is rearranged upon dsRNA binding. Leu198 in hOAS1 (Leu197 in pOAS1) is involved in a hydrophobic core, which is located close to the ATP binding pocket. Thus, the p.Leu198Val variant in hOAS1 (corresponding to p.Leu197Val in pOAS1) might impair ATP binding and enzymatic activity.

The free energy changes for each variant in a dsRNA-bound form of hOAS1 and an apo form of pOAS1 were calculated using the FoldX software through the YASARA interface.[23,24] After energy minimization with the "repair object" command, free energy change upon each variation was calculated with the "mutate residue" command through the YASARA interface. The FoldX calculation showed a marked increase in free energy associated with the p.Cys109Tyr variant in hOAS1 (p.Cys108Tyr in pOAS1) in the apo form of OAS1 (Figure 2B). This result suggested that p.Cys109Tyr likely disrupts the hydrophobic core of the apo form and the importance of this residue for regulation of enzymatic activity by dsRNA. FoldX predicted only a small impact of p.Ala76Val and p.Leu198Val on protein folding (Figure 2B).

The mechanisms by which the heterozygous mutations of *OAS1* described above cause PAP are unknown, and functional studies are currently underway. The OAS1 protein, encoded by *OAS1*, is a member of the 2-5A synthetase family essential for innate immune response against viral infection.[25–27] OASs are induced by interferons and use adenosine triphosphate in 2′-specific nucleotidyl transfer reactions to synthesize 2′,5′-oligoadenylates. These molecules activate latent RNase L, which results in degradation of both viral and endogenous RNA. In addition to antiviral activity, the OASs were reported to be involved in fundamental cellular functions, such as cell growth and differentiation, gene regulation, and apoptosis.[28] A single-nucleotide polymorphism (SNP), rs10774671, causing *OAS1* splicing variant p46 but not p48 and p52, is associated with increased susceptibility to plasma leakage and shock in individuals infected with dengue virus-2, indicating that immune overreaction could be triggered by the specific *OAS1* genotype, at least in dengue virus infection.[29] Although the functions of OAS1 on AMs have not been fully elucidated, expression of *OAS1* in AMs could be induced by oxidative stress.[30] Two SNPs are associated with severe acute respiratory syndrome (SARS) susceptibility: the G-allele of non-synonymous A/G SNP rs1131454 in exon 3 (p.Ser162Gly) located near the dsRNA binding domain and SNP rs2660 in the 3′ untranslated region of *OAS1*, possibly associated with expression of each transcriptional variant.[26,27] This association suggests the immune-modulating function of OAS1 protein especially in the respiratory system. Therefore, we speculated that the heterozygous mutations of *OAS1* observed in the three families, presumably gain-of-function mutations, might be associated with exaggerated immune reaction especially in AMs in response to viral infections, leading to dysfunction of AMs and impaired catabolism of lung surfactant.

There are a number of possible characteristic features of this disease, including infantile onset. All affected individuals were term infants and had no respiratory symptoms at birth. The onset of respiratory symptoms was distributed from 39 days to 5 months. The first symptoms appeared like a viral infection in most of the individuals, including C-II-1, who was positive for respiratory syncytial virus (RSV), cytomegalovirus, and subsequently coronavirus NL63 in sputum specimens during onset. Viral infections may trigger the onset of PAP via the mechanisms proposed above.

Hypogammaglobulinemia was observed in three affected individuals (A-II-4, B-II-1, and C-II-1) and was unclear in two individuals that died at 91 days (A-II-1) and 163 days (A-II-3). Three individuals that survived beyond the first year of life (A-II-4, B-II-1, and C-II-1) showed low levels of serum IgG, IgM, and IgA, although they had no B cell deficiency. Although the level of endogenous IgG was unknown due to repeated intravenous immunoglobulin (IVIG) administration, serum IgM and IgA levels increased gradually during the course of the disease. Hypogammaglobulinemia observed in affected individuals may be due to impaired B cell function by an as yet unknown mechanism caused by heterozygous *OAS1* mutations.

Small and non-foamy AMs were observed in four affected individuals (A-II-1, A-II-3, A-II-4, and C-II-1) and were undetermined in one individual (B-II-1). In contrast with the large and foamy AMs observed in APAP,[31] small and non-foamy AMs may indicate dysfunction of maturation and/or phagocytosis of AMs rather than impaired catabolism

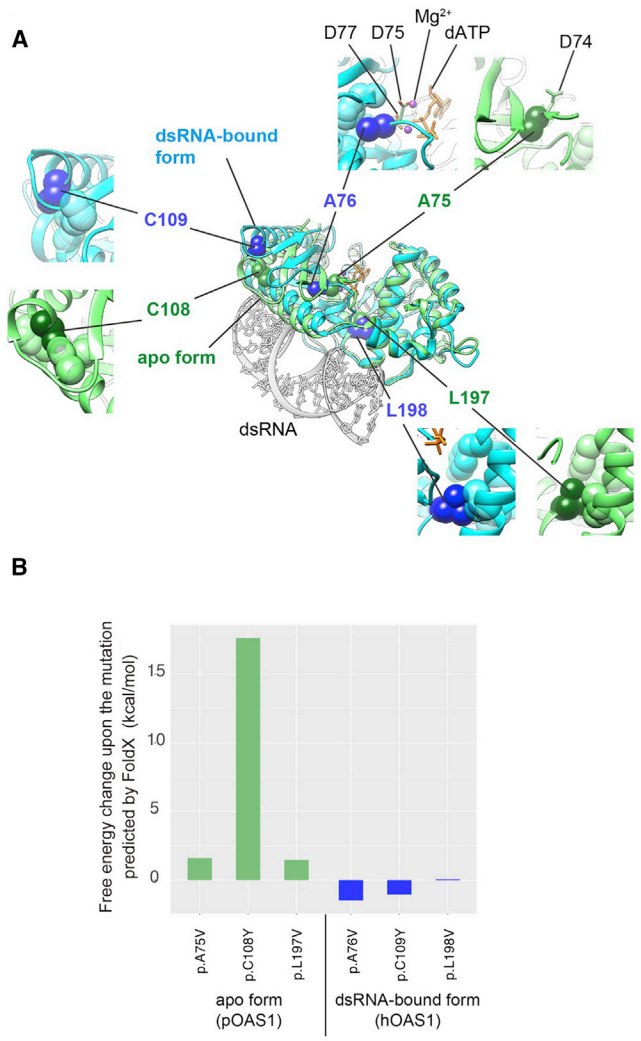

Figure 2. Impact of the Identified Variants on Protein Structure
(A) Mapping of the mutations on the crystal structures of a double-stranded RNA (dsRNA)-bound form of human oligoadenylate synthetase 1 (hOAS1) and an apo form of porcine OAS1 (pOAS1) (PDB: 4ig8 and 1px5, respectively). The superimposed structures of the dsRNA-bound (cyan) and apo (green) forms of OAS1 are presented as ribbon diagrams. The stick model is shown in gray. The altered residues are shown as van der Waals spheres in blue and dark green in the dsRNA-bound and apo forms, respectively. The substrate analog, 2′-deoxy ATP (dATP), and magnesium ions are shown as orange sticks and purple balls, respectively. Close-up views around the mutation sites are shown separately for the dsRNA-bound and apo forms. In the close-up views, some side chains of the hydrophobic residues around the mutation sites are shown as translucent spheres.
(B) The free energy changes associated with each variant in a dsRNA-bound form of hOAS1 and apo form of pOAS1 by the FoldX software are shown.

of phagocytosed lung surfactant. Although we performed BAL four times in A-II-4 and there were many CD14-positive small and non-foamy AMs every time, this finding was based on a single bronchoalveolar cell cytopathology specimen showing fewer than 20 cells in most of the individuals. Further studies in larger numbers of affected individuals with this disease are necessary.

Three individuals (A-II-4, B-II-1, and C-II-1) had overwhelming inflammation, which was not clear but was confirmed at autopsy in two individuals (A-II-1 and A-II-3). Splenomegaly, possibly related to hyperinflammation, was observed in four individuals (A-II-1, A-II-3, A-II-4, and C-II-1) before the initiation of replacement therapy with IVIG. Exogenous IgG improved respiratory symptoms and decreased systemic inflammatory responses in A-II-4, B-II-1, and C-II-1. However, AMs in bronchoalveolar lavage (BAL) fluid from A-II-4 under sequential IVIG showed no improvement in viability or phagocytosis of AMs (data not shown). Furthermore, A-II-4 showed gradual progression of PAP. Thus, immunoglobulin administration may be able to suppress uncontrolled inflammatory responses, without being able to improve dysfunction of AMs in terms of surfactant phagocytosis or catabolism. As inflammation plays an important role in the pathophysiology of PAP,[32] immunomodulation by IVIG may have some effect on the clinical course of PAP.

B-II-1 died from renal failure due to glomerulosclerosis following hematopoietic stem cell transplantation (HSCT). Glomerular diseases, including glomerulosclerosis, are increasingly observed especially in individuals with graft versus host disease after HSCT.[33] As renal biopsy was performed at the end stage of renal failure, it was difficult to determine whether glomerulosclerosis observed in B-II-1 was associated with HSCT. As another affected individual, A-II-4, showed proteinuria before initiation of monthly IVIG, OAS1 dysfunction itself could cause glomerular diseases. Long-term observation and accumulation of more individuals with this disease are necessary to evaluate this association.

Lung transplantation is a curative treatment for GPAP caused by mutations in genes encoding surfactant proteins or genes encoding a surfactant phospholipid transporter in alveolar type II epithelial cells.[34] On the other hand, HSCT is effective for GPAP caused by mutations in genes that could be responsible for surfactant catabolism in AMs.[35] In this study, two affected individuals (B-II-1 and C-II-1) received successful HSCT and recovered completely from PAP. C-II-1 has had cord blood engraftment for 2 years without any respiratory symptoms. It has been reported that AMs are derived from precursor cells in bone marrow.[36] Pulmonary transplantation of differentiated wild-type AMs derived from bone marrow in GM-CSF receptor-β-deficient mice showed long-term effectiveness due to proliferation of transplanted AMs.[37] Although IVIG could transiently improve the clinical condition, HSCT is the most effective therapy for this disease at present.

In summary, heterozygous mutations in *OAS1* cause infantile-onset PAP with hypogammaglobulinemia possibly caused by dysfunction of AMs. Infantile-onset leukocytosis without abnormal distribution, splenomegaly, and hyperreactivity were the most prominent findings. HSCT should be considered a curative treatment for this disease.

Supplemental Data

Supplemental Data include Supplemental Note, five figures, six tables, and Acknowledgments and can be found with this article online at https://doi.org/10.1016/j.ajhg.2018.01.019.

Acknowledgments

Professor J.A. Whitsett and Dr. W. Hull (Cincinnati Children's Hospital Medical Center, Cincinnati, OH) performed western blotting of SP-B in subject A-3 and measured concentrations of SP-A and SP-B in subject A-3, respectively. Professor H. Hasegawa (Tokyo Women's Medical University Medical Center East) supported BAL examination of subject C-II-1. This study was supported by grant for "Practical Research Project for Rare/Intractable Diseases" from the Japan Agency for Medical Research and Development #17930161 (2017-2018). Other financial supports were described in Supplemental Data.

Received: June 20, 2017
Accepted: January 25, 2018
Published: February 15, 2018

Web Resources

dbSNP, https://www.ncbi.nlm.nih.gov/projects/SNP/
ExAC Browser, http://exac.broadinstitute.org/
Human Genetic Variation Database, http://www.hgvd.genome.med.kyoto-u.ac.jp/
IGV, http://www.broadinstitute.org/igv/
Multiple Sequence Alignment, https://www.ebi.ac.uk/Tools/msa/clustalo/
MutationTaster, http://www.mutationtaster.org/
NHLBI Exome Sequencing Project (ESP) Exome Variant Server, http://evs.gs.washington.edu/EVS/
OMIM, http://www.omim.org/
PolyPhen-2, http://genetics.bwh.harvard.edu/pph2/
RefSeq, https://www.ncbi.nlm.nih.gov/RefSeq
SIFT, http://sift.bii.a-star.edu.sg/
SMART, http://www.smart.embl-heidelberg.de/

References

1. Jobe, A.H. (1993). Pulmonary surfactant therapy. N. Engl. J. Med. *328*, 861–868.
2. Whitsett, J.A., and Weaver, T.E. (2002). Hydrophobic surfactant proteins in lung function and disease. N. Engl. J. Med. *347*, 2141–2148.
3. Fitzgerald, M.L., Xavier, R., Haley, K.J., Welti, R., Goss, J.L., Brown, C.E., Zhuang, D.Z., Bell, S.A., Lu, N., McKee, M., et al. (2007). ABCA3 inactivation in mice causes respiratory failure, loss of pulmonary surfactant, and depletion of lung phosphatidylglycerol. J. Lipid Res. *48*, 621–632.
4. Uchida, K., Nakata, K., Trapnell, B.C., Terakawa, T., Hamano, E., Mikami, A., Matsushita, I., Seymour, J.F., Oh-Eda, M., Ishige, I., et al. (2004). High-affinity autoantibodies specifically eliminate granulocyte-macrophage colony-stimulating factor activity in the lungs of patients with idiopathic pulmonary alveolar proteinosis. Blood *103*, 1089–1098.
5. Trapnell, B.C., Whitsett, J.A., and Nakata, K. (2003). Pulmonary alveolar proteinosis. N. Engl. J. Med. *349*, 2527–2539.
6. Uchida, K., Nakata, K., Carey, B., Chalk, C., Suzuki, T., Sakagami, T., Koch, D.E., Stevens, C., Inoue, Y., Yamada, Y., and Trapnell, B.C. (2014). Standardized serum GM-CSF autoantibody testing for the routine clinical diagnosis of autoimmune pulmonary alveolar proteinosis. J. Immunol. Methods *402*, 57–70.
7. Tazawa, R., Hamano, E., Arai, T., Ohta, H., Ishimoto, O., Uchida, K., Watanabe, M., Saito, J., Takeshita, M., Hirabayashi, Y., et al. (2005). Granulocyte-macrophage colony-stimulating factor and lung immunity in pulmonary alveolar proteinosis. Am. J. Respir. Crit. Care Med. *171*, 1142–1149.
8. Handa, T., Nakatsue, T., Baba, M., Takada, T., Nakata, K., and Ishii, H. (2014). Clinical features of three cases with pulmonary alveolar proteinosis secondary to myelodysplastic syndrome developed during the course of Behçet's disease. Respir. Investig. *52*, 75–79.
9. Hamvas, A., Cole, F.S., and Nogee, L.M. (2007). Genetic disorders of surfactant proteins. Neonatology *91*, 311–317.
10. Spagnolo, P., and Bush, A. (2016). Interstitial lung disease in children younger than 2 years. Pediatrics *137*, e20152725.
11. Nogee, L.M., Garnier, G., Dietz, H.C., Singer, L., Murphy, A.M., deMello, D.E., and Colten, H.R. (1994). A mutation in the surfactant protein B gene responsible for fatal neonatal respiratory disease in multiple kindreds. J. Clin. Invest. *93*, 1860–1863.
12. Nogee, L.M., Dunbar, A.E., 3rd, Wert, S.E., Askin, F., Hamvas, A., and Whitsett, J.A. (2001). A mutation in the surfactant protein C gene associated with familial interstitial lung disease. N. Engl. J. Med. *344*, 573–579.
13. Tredano, M., Griese, M., Brasch, F., Schumacher, S., de Blic, J., Marque, S., Houdayer, C., Elion, J., Couderc, R., and Bahuau, M. (2004). Mutation of SFTPC in infantile pulmonary alveolar proteinosis with or without fibrosing lung disease. Am. J. Med. Genet. A. *126A*, 18–26.
14. Wambach, J.A., Casey, A.M., Fishman, M.P., Wegner, D.J., Wert, S.E., Cole, F.S., Hamvas, A., and Nogee, L.M. (2014). Genotype-phenotype correlations for infants and children with ABCA3 deficiency. Am. J. Respir. Crit. Care Med. *189*, 1538–1543.
15. Suzuki, T., Sakagami, T., Rubin, B.K., Nogee, L.M., Wood, R.E., Zimmerman, S.L., Smolarek, T., Dishop, M.K., Wert, S.E., Whitsett, J.A., et al. (2008). Familial pulmonary alveolar proteinosis caused by mutations in CSF2RA. J. Exp. Med. *205*, 2703–2710.
16. Suzuki, T., and Trapnell, B.C. (2016). Pulmonary alveolar proteinosis syndrome. Clin. Chest Med. *37*, 431–440.
17. Tanaka, T., Motoi, N., Tsuchihashi, Y., Tazawa, R., Kaneko, C., Nei, T., Yamamoto, T., Hayashi, T., Tagawa, T., Nagayasu, T., et al. (2011). Adult-onset hereditary pulmonary alveolar proteinosis caused by a single-base deletion in CSF2RB. J. Med. Genet. *48*, 205–209.
18. Hsu, A.P., McReynolds, L.J., and Holland, S.M. (2015). GATA2 deficiency. Curr. Opin. Allergy Clin. Immunol. *15*, 104–109.
19. Imagawa, E., Osaka, H., Yamashita, A., Shiina, M., Takahashi, E., Sugie, H., Nakashima, M., Tsurusaki, Y., Saitsu, H., Ogata, K., et al. (2014). A hemizygous GYG2 mutation and Leigh syndrome: a possible link? Hum. Genet. *133*, 225–234.
20. Yamada, M., Okura, Y., Suzuki, Y., Fukumura, S., Miyazaki, T., Ikeda, H., Takezaki, S., Kawamura, N., Kobayashi, I., and Ariga, T. (2012). Somatic mosaicism in two unrelated patients with X-linked chronic granulomatous disease characterized by the presence of a small population of normal cells. Gene *497*, 110–115.

21. Hartmann, R., Justesen, J., Sarkar, S.N., Sen, G.C., and Yee, V.C. (2003). Crystal structure of the 2′-specific and double-stranded RNA-activated interferon-induced antiviral protein 2′-5′-oligoadenylate synthetase. Mol. Cell *12*, 1173–1185.
22. Donovan, J., Dufner, M., and Korennykh, A. (2013). Structural basis for cytosolic double-stranded RNA surveillance by human oligoadenylate synthetase 1. Proc. Natl. Acad. Sci. USA *110*, 1652–1657.
23. Schymkowitz, J., Borg, J., Stricher, F., Nys, R., Rousseau, F., and Serrano, L. (2005). The FoldX web server: an online force field. Nucleic Acids Res. *33*, W382-8.
24. Van Durme, J., Delgado, J., Stricher, F., Serrano, L., Schymkowitz, J., and Rousseau, F. (2011). A graphical interface for the FoldX forcefield. Bioinformatics *27*, 1711–1712.
25. Justesen, J., Hartmann, R., and Kjeldgaard, N.O. (2000). Gene structure and function of the 2′-5′-oligoadenylate synthetase family. Cell. Mol. Life Sci. *57*, 1593–1612.
26. Hamano, E., Hijikata, M., Itoyama, S., Quy, T., Phi, N.C., Long, H.T., Ha, L.D., Ban, V.V., Matsushita, I., Yanai, H., et al. (2005). Polymorphisms of interferon-inducible genes OAS-1 and MxA associated with SARS in the Vietnamese population. Biochem. Biophys. Res. Commun. *329*, 1234–1239.
27. He, J., Feng, D., de Vlas, S.J., Wang, H., Fontanet, A., Zhang, P., Plancoulaine, S., Tang, F., Zhan, L., Yang, H., et al. (2006). Association of SARS susceptibility with single nucleic acid polymorphisms of OAS1 and MxA genes: a case-control study. BMC Infect. Dis. *6*, 106.
28. Mashimo, T., Simon-Chazottes, D., and Guénet, J.L. (2008). Innate resistance to flavivirus infections and the functions of 2′-5′ oligoadenylate synthetases. Curr. Top. Microbiol. Immunol. *321*, 85–100.
29. Simon-Loriere, E., Lin, R.J., Kalayanarooj, S.M., Chuansumrit, A., Casademont, I., Lin, S.Y., Yu, H.P., Lert-Itthiporn, W., Chaiyaratana, W., Tangthawornchaikul, N., et al. (2015). High anti-dengue virus activity of the OAS gene family is associated with increased severity of dengue. J. Infect. Dis. *212*, 2011–2020.
30. Kosmider, B., Messier, E.M., Janssen, W.J., Nahreini, P., Wang, J., Hartshorn, K.L., and Mason, R.J. (2012). Nrf2 protects human alveolar epithelial cells against injury induced by influenza A virus. Respir. Res. *13*, 43.
31. Golde, D.W. (1979). Alveolar proteinosis and the overfed macrophage. Chest *76*, 119–120.
32. Mukae, H., Ishimoto, H., Yanagi, S., Ishii, H., Nakayama, S., Ashitani, J., Nakazato, M., and Kohno, S. (2007). Elevated BALF concentrations of alpha- and beta-defensins in patients with pulmonary alveolar proteinosis. Respir. Med. *101*, 715–721.
33. Chang, A., Hingorani, S., Kowalewska, J., Flowers, M.E., Aneja, T., Smith, K.D., Meehan, S.M., Nicosia, R.F., and Alpers, C.E. (2007). Spectrum of renal pathology in hematopoietic cell transplantation: a series of 20 patients and review of the literature. Clin. J. Am. Soc. Nephrol. *2*, 1014–1023.
34. Palomar, L.M., Nogee, L.M., Sweet, S.C., Huddleston, C.B., Cole, F.S., and Hamvas, A. (2006). Long-term outcomes after infant lung transplantation for surfactant protein B deficiency related to other causes of respiratory failure. J. Pediatr. *149*, 548–553.
35. Lachmann, N., Happle, C., Ackermann, M., Lüttge, D., Wetzke, M., Merkert, S., Hetzel, M., Kensah, G., Jara-Avaca, M., Mucci, A., et al. (2014). Gene correction of human induced pluripotent stem cells repairs the cellular phenotype in pulmonary alveolar proteinosis. Am. J. Respir. Crit. Care Med. *189*, 167–182.
36. Nakata, K., Gotoh, H., Watanabe, J., Uetake, T., Komuro, I., Yuasa, K., Watanabe, S., Ieki, R., Sakamaki, H., Akiyama, H., et al. (1999). Augmented proliferation of human alveolar macrophages after allogeneic bone marrow transplantation. Blood *93*, 667–673.
37. Suzuki, T., Arumugam, P., Sakagami, T., Lachmann, N., Chalk, C., Sallese, A., Abe, S., Trapnell, C., Carey, B., Moritz, T., et al. (2014). Pulmonary macrophage transplantation therapy. Nature *514*, 450–454.

The American Journal of Human Genetics, Volume *102*

Supplemental Data

Heterozygous Mutations in *OAS1* Cause Infantile-Onset Pulmonary Alveolar Proteinosis with Hypogammaglobulinemia

Kazutoshi Cho, Masafumi Yamada, Kazunaga Agematsu, Hirokazu Kanegane, Noriko Miyake, Masahiro Ueki, Takuma Akimoto, Norimoto Kobayashi, Satoru Ikemoto, Mishie Tanino, Atsushi Fujita, Itaru Hayasaka, Satoshi Miyamoto, Mari Tanaka-Kubota, Koh Nakata, Masaaki Shiina, Kazuhiro Ogata, Hisanori Minakami, Naomichi Matsumoto, and Tadashi Ariga

SUPPLEMENTAL NOTE

CASE REPORT

We found five individuals (A-II-1, A-II-3, A-II-4, B-II-1, and C-II-1) with infantile-onset pulmonary alveolar proteinosis (PAP) with hypogammaglobulinemia from three unrelated families (Figure S1 and Table 1).

[A-II-1], male

This male infant was born to non-consanguineous parents (Figure S1A and Table 1). His clinical course was reported previously.[1] Briefly, he did not show respiratory problem at birth, but died at 91 days of age following sucking difficulty since 9 days of age, hospitalization with a diagnosis of pneumonia at 39 days of age, and progressive respiratory failure requiring mechanical ventilation since 55 days of age. Surfactant replacement was not effective for his respiratory failure. Autopsy revealed PAP, but the cause of PAP was unknown.

[A-II-2], male

He was healthy (Figure S1A).

[A-II-3], male

This male infant showed no respiratory problems at birth, but was hospitalized for fever, cough, and failure to thrive at 39 days of age with a diagnosis of pneumonia (Figure

S1A and Table 1). A diagnosis of PAP was made after bronchoalveolar lavage (BAL) examination at 100 days of age following supplemental oxygen requirement since 86 days and mechanical ventilation since 92 days of age. Steroid administration, inhalation of nitric oxide, and extracorporeal membrane oxygenation were ineffective, and he finally died of respiratory failure at 163 days of age before bone marrow engraftment following hematopoietic stem cell transplantation (HSCT) with his father's bone marrow at 151 days of age. Autopsy confirmed PAP and indicated cytomegalovirus infection in the lung. Cytomegalovirus infection was considered as a complication at the end stage of his clinical course. No abnormalities in *GMCSF*, the gene encoding GM-CSF, were detected in genomic DNA from his peripheral white blood cells (WBCs). Surfactant protein (SP)-B was detectable in the BAL fluid. No significant anti-GM-CSF antibody was detected in freeze-stored BAL.

[A-II-4], female

The clinical course before 5 years of age (Figure S1A and Table 1) was reported previously as GPAP with hypogammaglobulinemia.[2] Briefly, similar to the two elder brothers affected by GPAP, this female infant did not have respiratory symptoms at birth. However, she became febrile (40°C) unresponsive to antibiotics and had generalized skin rash at 23 days of age. Abnormal chest X-ray and CT findings were first observed at 42 days of age as shown in Figures S2A and S3A, respectively. Her respiratory dysfunction was repeatedly responsive to monthly intravenous

immunoglobulin (IVIG) administration. She required hospitalization 19 times over 10 years from 1 to 10 years of age for treatment of recurrent infections, mainly by viruses, including pneumonia, bronchitis, gastroenteritis, peritonitis, otitis media, and cystitis. She showed excessively strong reaction to each infection. Although IVIG was effective to improve respiratory function and overcome infection, she required home oxygen therapy since 8 years of age (Figure S3B). Finally, she died of respiratory failure at 11.3 years of age while awaiting HSCT (Figure S2C). Autopsy showed alveoli diffusely occupied with PAS-positive materials and small and non-foamy alveolar macrophages (AMs) (Figures S5A–D).

Her serum levels of SP-A (up to 154 ng/mL), Krebs von den Lungen-6 (KL-6) (up to 46190 U/mL), IgM (up to 60 mg/dL), and IgA (up to 57 mg/mL) were elevated at 11 years old. SP-D level was consistently within the normal range during the course. The serum IgG level showed a trough of 102 mg/dL at 102 days of age, and WBC count was consistently high, ranging from 10000 to 86000 /μL throughout her clinical course. Splenomegaly and proteinuria were observed before monthly IVIG but disappeared after initiation of this therapy. BAL fluid (Figure S4A) contained acidophilic sediments that were stained strongly with PE10 (anti-SP-A antibody), high levels of SP-A (10 μg/mL; reference 1.3–5.2 μg/mL) and SP-B (700 ng/mL) with normal SP-A:SP-B ratio, GM-CSF (17.7 pg/mL), and macrophage colony stimulating factor (M-CSF) (70840 pg/mL). BAL fluid contained large number of small and non-foamy AMs (Figure S4B). The AMs showed weak staining for PE10 and CD14 but

were quite different from large and foamy AMs observed in individuals with autoimmune PAP (APAP). Her AMs cultured in medium even with GM-CSF died within a shot time. No significant anti-GM-CSF antibodies were detected in her sera

[B-II-1], female

The clinical course of this female infant was reported previously.[3] Briefly, she was born with no respiratory symptoms, but was hospitalized due to vesicles on the face, buttocks, and extremities at 29 days of age (Figure S1B and Table 1). Leukocytosis and low serum levels of IgG (101 mg/dL), IgM (3 mg/dL), and IgA (2 mg/dL) were observed on admission. She then presented with tachypnea without cough at 2 months of age. Confluent consolidations were seen in both lungs on chest CT at the age of 4 months (Figure S3C). The findings of BAL fluid were consistent with the diagnosis of PAP (Figure S4C). As AM dysfunction was considered, HSCT with cord blood was performed at 8 months of age.[3] Respiratory function improved markedly 21 days after myeloid engraftment followed by no dense consolidations on chest CT 2 months after HSCT (Figure S3D). Although she had no recurrence of respiratory dysfunction, she was complicated by reactivated cytomegalovirus infection and finally died from renal failure with histological findings of focal glomerulosclerosis at 3 years of age.

[C-II-1], female

The clinical course of this female infant was also reported previously.[3] Briefly, she was

born with no respiratory symptoms, but was hospitalized at 5 months of age for pneumonia caused by respiratory syncytial virus (RSV) requiring mechanical ventilation for 10 days (Figure S1C and Table 1). In addition, she suffered from cytomegalovirus and subsequently coronavirus NL63 infection. She showed low serum levels of IgG (103 mg/dL), IgM (11 mg/dL), and IgA (3 mg/dL). Although sequential IVIG and subcutaneous immunoglobulin appeared to be effective, she had persistent respiratory symptoms and progressive consolidation on chest X-ray and CT (Figures S2D and S3E). Anti-GM-CSF antibody was not detected in the serum. BAL fluid at 8 months of age contained PAS-positive acidophilic material (Figure S4D), small and non-foamy AMs (Figure S4E), and elevated levels of SP-A (> 2 μg/mL) and SP-D (8240 ng/mL). These findings were consistent with PAP. HSCT with cord blood performed at 11 months of age was effective. She left hospital with no respiratory symptoms at 16 months of age (Figure S3F) after overcoming graft versus host disease.

ACKNOWLEDGEMENTS

This study was supported by grants for; Research on Measures for Intractable Diseases; Comprehensive Research on Disability Health and Welfare, the Strategic Research Program for Brain Science; Initiative on Rare and Undiagnosed Diseases in Pediatrics and Initiative on Rare and Undiagnosed Diseases for Adults from the Japan Agency for Medical Research and Development; Grants-in-Aid for Scientific Research on

Innovative Areas (Transcription Cycle) from the Ministry of Education, Science, Sports, and Culture of Japan; Grants-in-Aid for Scientific Research (B) from the Japan Society for the Promotion of Science; Creation of Innovation Centers for Advanced Interdisciplinary Research Areas Program in the Project for Developing Innovation Systems from the Japan Science and Technology Agency; grants from Ministry of Health, Labor and Welfare; the Takeda Science Foundation; the Yokohama Foundation for Advancement of Medical Science; and the Hayashi Memorial Foundation for Female Natural Scientists.

SUPPLEMENTAL FIGURES

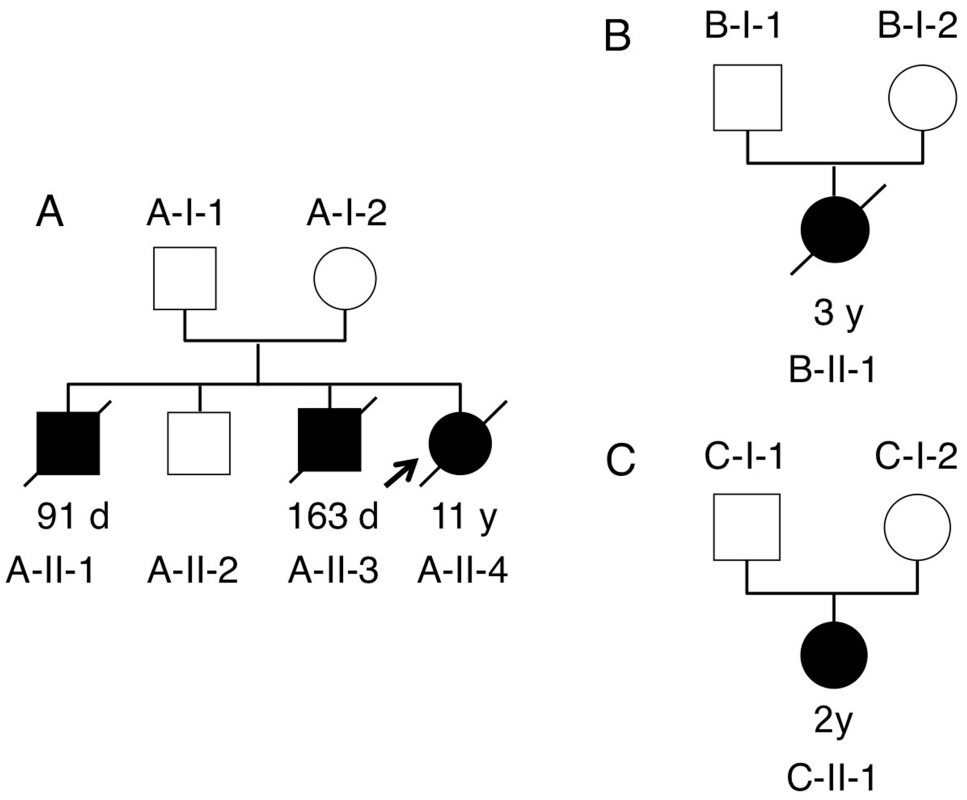

Figure S1. Pedigrees of the three families

A (family A): Three siblings, two boys and one girl, were affected.

B (family B): B-II-1 was affected.

C (family C): C-II-1 was affected.

All affected individuals were born to non-consanguineous parents.

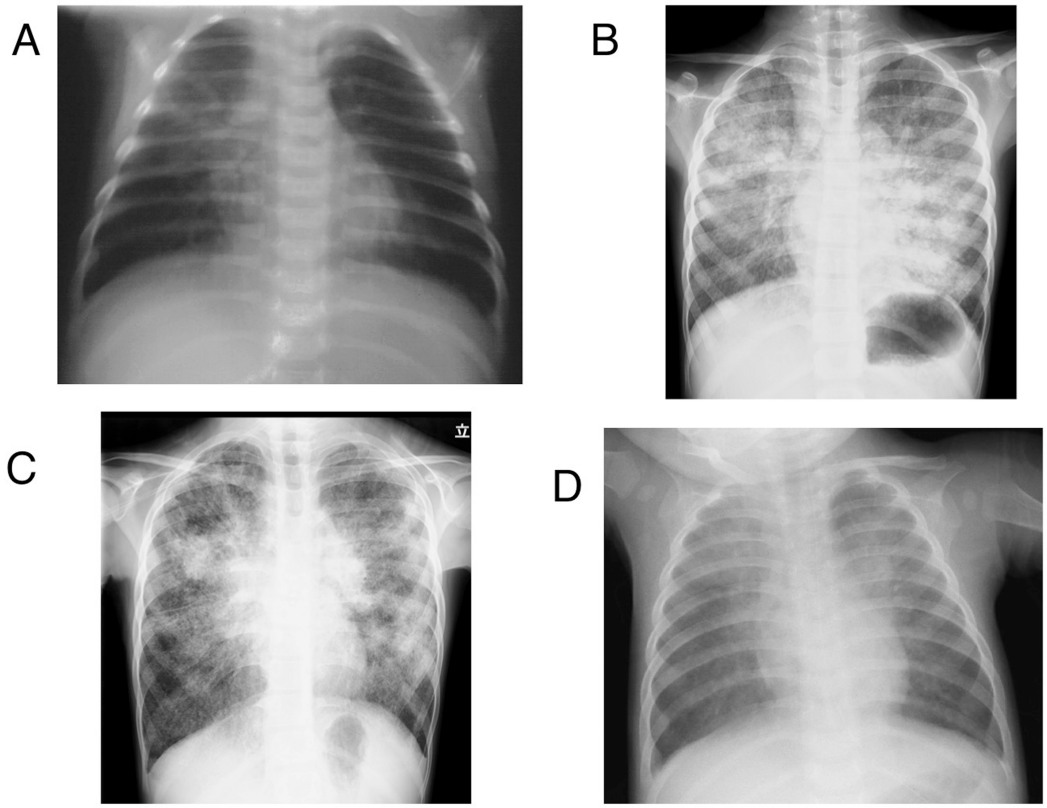

Figure S2. Chest X-ray findings

A (A-II-4, 42 days): Mild consolidation was first observed in the right lung.

B (A-II-4, 8 years): Her respiratory status and oxygenation function gradually deteriorated and needed home oxygen therapy at 8 years old.

C (A-II-4, 11 years): This X-ray was at the end stage of respiratory failure on noninvasive positive pressure ventilation. Diffuse infiltrations and bilateral silhouette signs were observed.

D (C-II-1, 24 days): Diffuse opacity in her lung increased gradually.

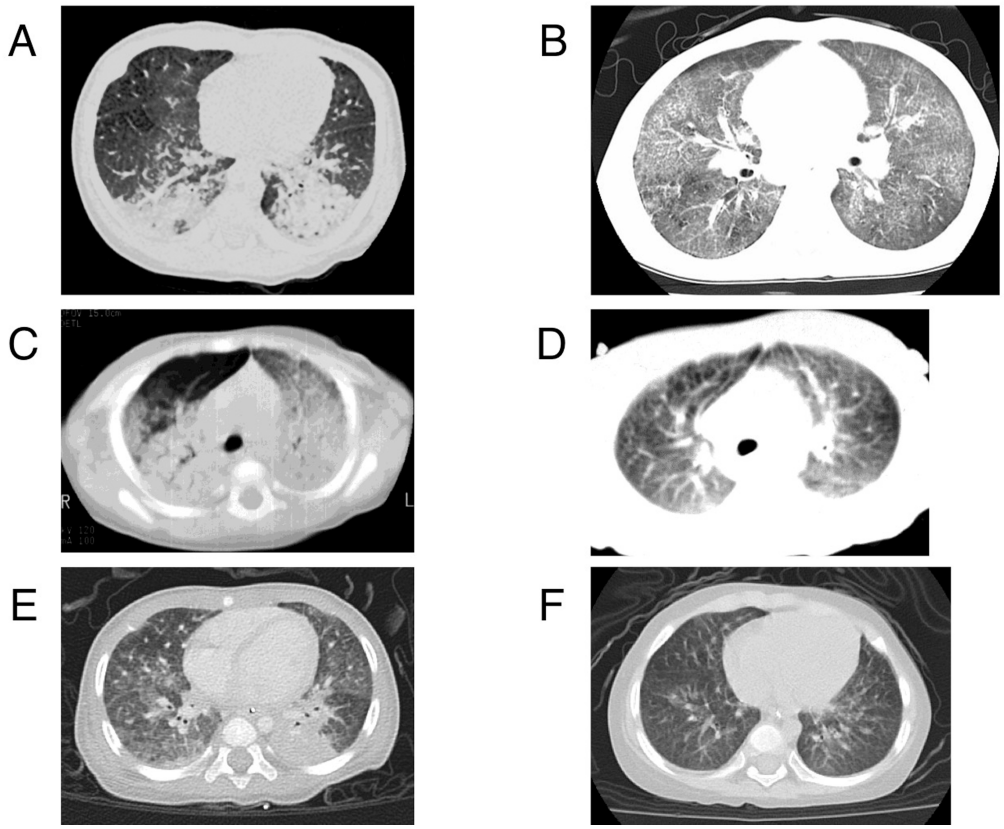

Figure S3. Chest CT findings

A (A-II-4, 42 days): Apparent consolidation was seen in both dependent sides.

B (A-II-4, 9 years): Ground glass opacity, crazy paving pattern, and geographic opacity, findings typical of PAP, were observed.

C (B-II-1, 5 months): Severe consolidation on both dependent sides was observed.

D (B-II-1, 10 months): Consolidation on chest CT had clearly disappeared 2 months after hematopoietic stem cell transplantation (HSCT) with cord blood.

E (C-II-1, 9 months): Diffuse consolidation was observed.

F (C-II-1, 2 years): Consolidation had disappeared on follow up chest CT after HSCT.

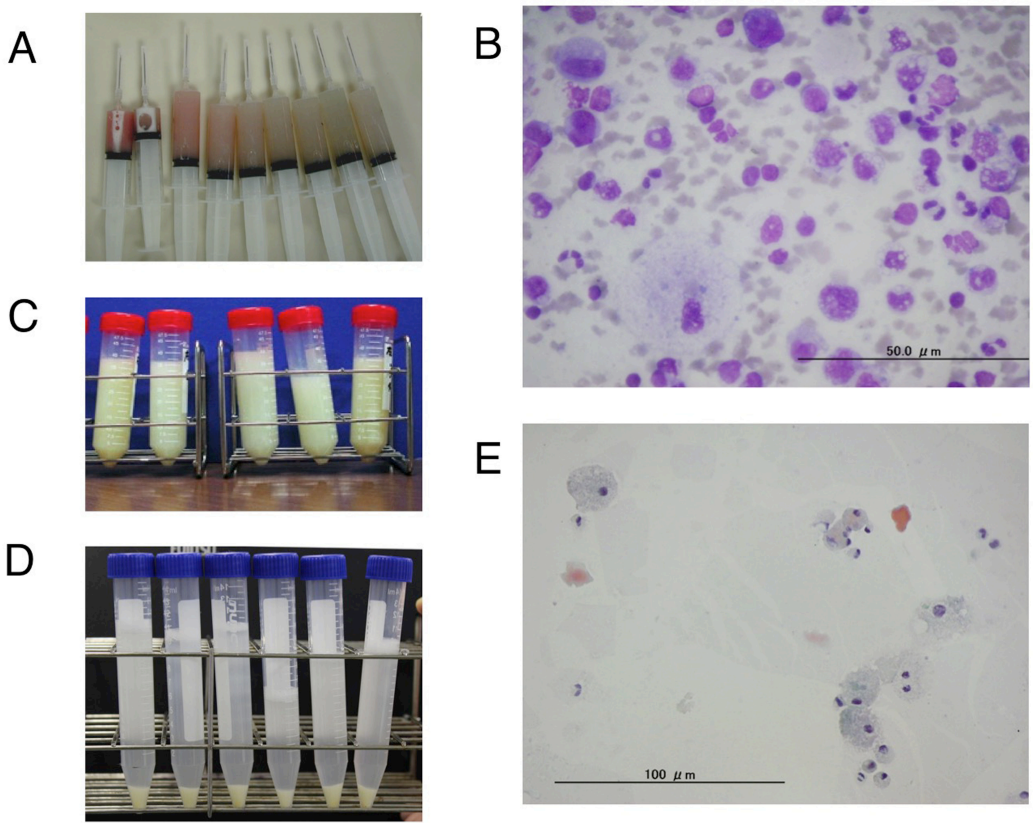

Figure S4. Findings in BAL fluid

A (A-II-4, 42 days): BAL fluid obtained from the right lung at 66 days of life was milky white in appearance and contained flocculent precipitates, which stained positively with periodic acid-Schiff stain.

B (A-II-4, 42 days): Cytospin slide staining of BAL fluid with hematoxylin and eosin (HE). AMs were various in size and there were many CD14-positive small and non-foamy AMs.

C (B-II-1, 4 months): BAL fluid had a milky white appearance and contained abundant precipitates.

D (C-II-1, 9 months): BAL fluid obtained from the right lung at 9 months was milky

white and precipitates were observed after centrifugation.

E (C-II-1, 9 months): Cytospin staining of BAL fluid with Papanicolaou staining. AMs in BAL fluid were small and non-foamy.

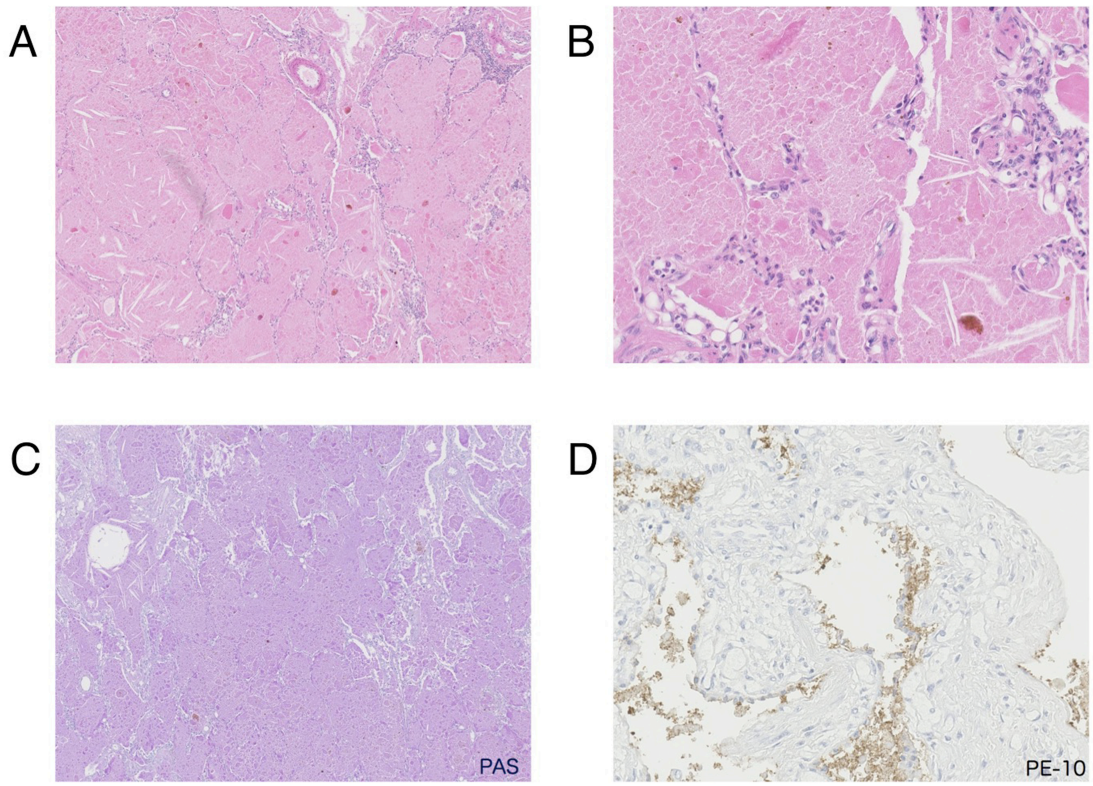

Figure S5. Histological findings of the lung of A-II-4

A: HE staining of the lung tissues showed alveolar spaces filled with proteinaceous material, compatible with PAP (low magnification).

B: HE staining of lung tissues showed small and non-foamy AMs (high magnification).

C: The materials filling the alveolar spaces were positive for PAS.

D: Materials in alveolar spaces and AMs were not stained by PE-10 (anti-SP-A).

SUPPLEMENTAL TABLES

Table S1. Oligonucleotide primer sets for *OAS1*

	Forward	Reverse
Exon 1	AATTCAGCACTGGGATCAGG	GCACCCTGGGTTCTAGGTTT
Exon 2	ATTTAGGGAGGTTTGCCTCA	CCCACCCTGCTTTAGAGAGA
Exon 3	CTGGGTCTGCTGCACTTTTC	CCCTCCTCTTCCCTTCACTC
Exon 4	GGATTCGTTCCAAGGAAACTT	CACAGGGTTGGAGGTAGGTG
Exon 5	GAGCCCTTCCTCATGTTCTG	CAAACCCCACCATTACACAA
Exon 6	TCCAGATGGCATGTCACAGT	TGGCTCTGTGCCTTGAAGTT

The coding and flanking intronic regions of three transcriptional variants of *OAS1* (RefSeq NM_016816.3, NM_002534.3, and NM_001032409.2) were amplified by these primer sets.

Table S2. Exonic sequence coverage by whole exome sequencing in family A

ID	Sample Type	Total (bps)	Mean depth	≥ ×5 (%)	≥ ×10 (%)	≥× 20 (%)	PCR duplication (%)
Father (A-I-1)	WGA	3,683,035,312	110.03	83.1	76.1	66.6	13.0
Mother (A-I-2)	WGA	3,849,394,706	115	83.5	76.9	67.9	13.3
Affected (A-II-1)	WGA	3,822,951,097	114.21	90.1	84.8	76.1	19.5
Unaffected (A-II-2)	WGA	3,510,531,591	104.88	80.7	73.7	64.6	10.7
Affected (A-II-3)	WGA	3,626,875,251	108.36	89.3	83.8	75	28.7
Unaffected (A-II-2)	EBV-LCL	4,000,057,549	119.5	96.1	94.8	91.2	12.8
Affected (A-II-4)	EBV-LCL	3,186,587,499	95.2	95.6	93.8	88.7	13.3

WGA, whole genome amplification; EBV-LCL, Epstein-Barr virus-transformed lymphoblastoid cell line

Table S3. Priority scheme of homozygous variants

Criteria for filtering	Variant counts
Total variants	4,903
Remove synonymous	3,289
In-house exome data ($n \leq 1/153$)	1,424
MAF ≤ 0.01 in ESP5400	1,373
Outside Segmental duplication	1,287
Commonly shared homozygous variants among three affected children	0

Table S4. Priority scheme of compound heterozygous variants

Criteria for filtering	Variant counts
Total variants	4,903
Remove synonymous	3,289
In-house exome data ($n \leq 1/153$)	1,424
MAF ≤ 0.01 in ESP5400	1,373
Outside segmental duplication	1,287
Commonly shared heterozygous variants among three affected children	116
Commonly shared compound heterozygous variants among three affected children	0

Table S5. Priority scheme of *de novo* variants

Filtering criteria	Variant counts
Total variants	4,903
Remove synonymous	3,289
Remove in-house exome data (n = 153)	1,086
Not registered in dbSNP 135	623
Not registered in ESP5400	595
Outside Segmental duplication	570
Not observed in both parents and unaffected sibling	212
Commonly shared heterozygous variants among three affected children	1

Table S6. Read counts for *OAS1* mutation (c.227C>T) by deep sequencing

	Father		Mother	
Called base	Read count	(%)	Read count	(%)
A	326	0.10	328	0.09
T	361	0.12	13,512	3.81
G	70	0.02	54	0.02
C	312,759	99.72	340,680	96.05
N	117	0.04	132	0.04
Total	313,633	100.00	354,706	100.00

SUPPLEMENTAL REFERENCES

1. Shimizu, H., Kaneko, K., Arakawa, H., Yoshida, N., Igarashi, Y., Nakamura, T., Oka, T., Itoyama , S., and Y., O. (1998). Measurement of pulmonary surfactant proteins in sera in congenital alveolar proteinosis. (in Japanese with English abstract). J. Jpn. Pediatr. Soc. 102, 568–575.
2. Cho, K., Nakata, K., Ariga, T., Okajima, S., Matsuda, T., Ueda, K., Furuta, I., Kobayashi, K., and Minakami, H. (2006). Successful treatment of congenital pulmonary alveolar proteinosis with intravenous immunoglobulin G administration. Respirology 11, S74–77.
3. Tanaka-Kubota, M., Shinozaki, K., Miyamoto, S., Yanagimachi, M., Okano, T., Mitsuiki, N., Ueki , M., Yamada, M., Imai, K., Takagi, M., et al. Hematopoietic stem cell transplantation for pulmonary alveolar proteinosis associated with primary immunodeficiency disease. Int. J. Hematol. (in press).